Received: 19 June 2016 | Revised: 10 August 2016 | Accepted: 12 August 2016

DOI 10.1002/qua.25285

FULL PAPER

WILEY International Journal of QUANTUM CHEMISTRY

Depicting electronic distributions from accurate computational first principles: On the relationship between the complex patterns of bonding interaction and the back-donation phenomenon

Rosana M. Lobayan[1] | Roberto C. Bochicchio[2] | Carlos Pérez del Valle[3]

[1]Departamento de Física, Facultad de Ciencias Exactas, Naturales y Agrimensura Universidad Nacional del Nordeste, Corrientes 3400, Argentina

[2]Departamento de Física, Facultad de Ciencias Exactas y Naturales, Universidad de Buenos Aires and IFIBA, CONICET, Ciudad Universitaria, Buenos Aires 1428, Argentina

[3]Département de Chimie Moléculaire, Université Grenoble Alpes, Grenoble Cedex, Grenoble F-38000, France

Correspondence
Roberto C. Bochicchio, Departamento de Física, Facultad de Ciencias Exactas y Naturales, Universidad de Buenos Aires, Pab. 1, Ciudad Universitaria, Buenos Aires, Argentina.
Email: rboc@df.uba.ar

Abstract

A detailed theoretical description of metal–ligand interactions in the case of the simple isoelectronic transition metal series Ni, Cu^{+}, Zn^{2+} and one C_2H_4 ligand is presented. This task is performed in terms of the local and nonlocal topology-based formalisms of the electronic density and its decomposition into paired and unpaired contributions. The analysis is mainly focused on the nature of the carbon–metal interactions under the traditional chemical back-donation phenomena and the relationship with the existence of two-electron three-center (2e-3c) complex patterns of bonding, that is, 2e-3c atomic interactions. For these simple prototypical systems, which seem to be adequate examples to describe the topologic features of such electron distribution in terms of the density point of view, both phenomena, that is, the back-donation and the 2e-3c interactions, are mutually exclusive.

KEYWORDS

back-donation, complex patterns of bonding, electronic density, electronic distribution, topology

1 | INTRODUCTION

The electron density ρ contains the complete information about a molecular system.[1] It may be obtained from several methods of quantum chemistry ranging from the very state function by contraction of density matrices[2] to Kohn–Sham density functional theory.[3] The advent of topologic theories of the density[4,5] and the computational tools enable a more detailed description of the electron distribution and a precise understanding of the interactions between atoms leading to detect the onset of complex patterns of bonding.[6] For this goal, a precise definition of the system composed of atoms or a group of them, that is, moieties, is needed. Hence, it merits the introduction of the quantum theory of atoms in molecules (QTAIM) concept giving a definite structure to the system. In its most rigorous form, it is based in the Lagrangian quantum mechanics formulation, permits to define an atom in a molecular framework.[4,5] These techniques permit the treatment of all type of molecular structure whatever their nature, that is, ionic, covalent, multicenter, etc., in the same footing and thus to go beyond the description of the classical structures. Consequently, on one side, because of the lack of a rigorous definition of the concept chemical bond beyond empirical frameworks[7] and on the other side, the general validity of the present methodology of study lead us to refer the former as chemical interactions which permit unify the wide variety of which is called chemical bond. To reach this goal, we introduced an appropriate methodology based in the exact decomposition of the electron density into paired ($\rho^{(p)}(\mathbf{r})$) and unpaired ($\rho^{(u)}(\mathbf{r})$) contributions, each of them with a different and definite physical character.[8,9] The application of this analysis to distinct type of distributions permitted to interpret and further classify the electron distributions by means of the type of interactions they undergo.[6] Therefore, a quantum version of the pairing Lewis model and its deviations is allowed to be interpreted in this sense. In previous works, we applied this formalism to classical structures of chemical compounds as well as to more complex systems ranging from electron deficient compounds like boron hydrids, molecular organic ions, and simple organo-metallic systems to metalloid clusters.[6,10] The analysis and discussion of the results of the

whole set of mentioned type of systems by means of this technique enables us not only to perform a detailed description of the electron distribution but also detect complex patterns of bonding as those resulting from the two-electron three-center (2e-3c) interaction mechanisms. Hence, this methodology provides a strong support for the description and understanding of the atomic interaction phenomena. In this work, chemical bonding interactions in transition metal (TM)–ligand (L) complexes[11–14] are described and interpreted from the density point of view instead of the orbital view. Its most naive interpretation has often been considered to be of electrostatic interaction nature. Nonetheless, the most of their theoretical studies have been based on interpretations of the state function by analyzing the molecular orbitals and the attention has been concentrated on the donation & back-donation process stressing the process of charge transfer in the popular semiempirical Dewar–Chatt–Duncanson model.[12–16] Although in the present work will refer to this model, there is another orbital alternative approach based on the ideas of quantum information theory particularly those of multiorbital correlations[17,18] showing similar results at least for the Ni-ethene system[19,20] to the reported in the present work.

We mainly focus our attention in two aspects. On one side, the physical meaning of the density description for the well-established molecular orbital models of donation and back-donation phenomena which consists in the transfer of electrons from the L to the TM (here in after denoted as Me) and in the opposite direction, from the Me to the L, respectively.[15] On the other side, the onset of 2e-3c bonding interactions as complex patterns of bonding within these type of systems[6]; and the relationships between both mentioned aspects, that is, the 2e-3c interactions and the back-donation phenomena. Such phenomena regarded as the whole rearrangement of the electronic charge distribution includes polarization, exchange repulsion, and charge transfer.[11–14,16] The scenario for the present research is to apply our topologic methodology to the isoelectronic series of TM-alkene ligand interactions, that is, $Me^{p+}(C_2H_4)$ with $Me^{p+} = Ni, Cu^{+}, Zn^{2+}$. The election of these systems has been supported on their existence as complexes,[21–23] their simplicity, which permits to understand the electronic structure of these phenomena and the fact that they have been suggested as candidates for undergoing back-donation phenomena.

It is worthy to emphasize that the tools we use here perform an attempt to extract the information contained in the *ab initio* *N*-electron state function at any theoretical level of approximation from their associated electron density and not from the use of molecular orbital models. To this end, such information may be transferred toward the fundamental chemical concepts that will be carried out by determining the classical descriptors of chemistry, as atomic charges, covalent bond orders, valences among others and the nonclassical 2e-3c populations (integrated or nonlocal formulation),[24–26] and by local descriptors like critical points of the electron densities, that is, total, paired, and unpaired ones, and/or of their Laplacian fields (local formulation).[8–10] These two formulations are complementary each other to assess the information contained in the density and hence allowing an electronic description of the systems in a qualitative and also a quantitative manner. The treatment of the chosen systems provides a valuable experience for both, the application of the density decomposition model and the essential role of electron correlation effects on the electron distribution.

The main goal of this report is to study the capability of these density tools in the topologic framework, to describe the interactions in the electron distributions undergoing back-donation phenomena and its relationships with 2e-3c type nonconventional patterns of bonding.[26]

The organization of this article is as follows. The Second section is dedicated to give a brief report of the theoretical framework of the methodology, partitioning of the electron density, relationships between the density gradients and Laplacian of both fields, as well as the tools used to carry out the studies of topologic population analysis. The Third section is devoted to describe the computational details, the results and the discussion. The Forth Section collects the concluding remarks.

2 | THEORETICAL FRAMEWORK

The diagonal elements of the contracted 2-particle reduced density matrix ${}^2D$[2] (2-RDM) straightforwardly leads to the density $\rho(\mathbf{r})$ decomposition of an *N*-electron system into two contributions of different nature, the effectively paired $\rho^{(p)}(\mathbf{r})$ and effectively unpaired $\rho^{(u)}(\mathbf{r})$ densities, respectively. Therefore, it is expressed as $\rho(\mathbf{r}) = \rho^{(p)}(\mathbf{r}) + \rho^{(u)}(\mathbf{r})$ with[8,9]

$$\rho^{(p)}(\mathbf{r}) = \frac{1}{2}\int d\mathbf{r}'\, {}^1D(\mathbf{r}|\,\mathbf{r}')\,{}^1D(\mathbf{r}'|\,\mathbf{r}),\ \rho^{(u)}(\mathbf{r}) = \frac{1}{2}\,u(\mathbf{r}|\,\mathbf{r}) \tag{1}$$

where ${}^1D(\mathbf{r}|\mathbf{r}')$ stands for first-order reduced density matrix (1-RDM) in the spin-free representation.[2,27,28] The integration of ρ over the whole space, that is, $tr({}^1D) = \int d\mathbf{r}\, {}^1D(\mathbf{r}|\mathbf{r}) = \int d\mathbf{r}\, \rho(\mathbf{r}) = N$ (summation of the diagonal elements) is the trace operation which results in the number of electrons in the system, *N*.[2,27,28] The effectively unpaired density matrix defined by $u(\mathbf{r}|\,\mathbf{r}') = 2\,{}^1D(\mathbf{r}|\,\mathbf{r}') - {}^1D^2(\mathbf{r}|\,\mathbf{r}')$ with ${}^1D^2(\mathbf{r}|\,\mathbf{r}') = \int d\mathbf{r}''\, {}^1D(\mathbf{r}|\,\mathbf{r}'')\,{}^1D(\mathbf{r}''|\,\mathbf{r}')$ has its associated density, that is, the effectively unpaired density, defined by $u(\mathbf{r}|\,\mathbf{r})$.[8,9,27,28] The physical meaning of these densities are related to the difference of the orbital occupation from the double occupancy due to the spin state and the correlation effects. Both contributions, paired and unpaired allow to show how correlation effects modify the double occupancy of the molecular (or natural) orbitals. The detailed description of the unpaired density $\rho^{(u)}(\mathbf{r})$ shows that it has two sources, one of them comes from the spin density (only present in non-singlet states) and the other corresponds are exclusively due to the correlation effects[29] and provides the local finer details of the electron distribution. It is intrinsically zero[30–33] for single determinant state functions having all doubly occupied orbitals. For the nonequilibrium conformations, like atomic dissociation of molecules their behavior clarifies its close relation to the correlation-entanglement phenomena.[34]

The localization of the critical points **cp**s of the density (first spatial derivatives), the local accumulation/depletion in their surroundings (Laplacian function), and the breakdown of the symmetries along the cartesian axis (ellipticity) are the fundamental topologic indicators

containing the information which defines the nature of atomic interactions.[4,5] The density **cp**s are evaluated by the gradient of the field throughout the relation

$$\nabla\rho(\mathbf{r})|_{\mathbf{r}^c}=0, \nabla\rho^{(p)}(\mathbf{r})|_{\mathbf{r}^c}+\nabla\rho^{(u)}(\mathbf{r})|_{\mathbf{r}^c}=0 \tag{2}$$

where $\mathbf{r}^c=\{\mathbf{r}_i^c; i=1,\ldots M\}$ indicates the set of critical points of $\rho(\mathbf{r})$. Note that the $\nabla\rho^{(p)}(\mathbf{r})|_{\mathbf{r}^c}=-\nabla\rho^{(u)}(\mathbf{r})|_{\mathbf{r}^c}$ relation, physically means that both densities cannot increase their values in the same direction. The **cp**'s are mathematically classified by the two numbers (*r*,*s*), where *r* is the *rank* (number of nonvanishing eigenvalues of the Hessian matrix of $\rho(\mathbf{r})$) and *s* the *signature* (sum of the signs of its eigenvalues). In the three dimensional physical space, they are classified as: nuclear critical points $(3,-3)$ (**ncp**), which localize a local maximum very close to the nuclear positions and stands for the expected concentration of electron population close to the physical nuclei; the existence of a bond critical point (**bcp**) $(3,-1)$ establishes a bonding interaction between two atoms and the concentration of the electron density on it, the idea of its strength.[4,5] The onset of the other type of points, that is, *ring* (**rcp**) and *cage* (**ccp**), noted as $(3,+1)$ and $(3,+3)$, respectively, indicates a more complex molecular structure relating the electron structure with the geometrical conformation.[4,5] The density, as any other function of the space coordinates, is described not only by the location of its **cp**s and its value but also by the behavior at its surroundings which states its locally depletion or concentration. This behavior is described by the modulus and sign of the Laplacian field.[4,5] It is worthy to note that each of the densities are allowed to concentrate or deplete simultaneously at the neighborhood of a **cp** as it is indicated by the Laplacian relation $\nabla^2\rho(\mathbf{r})|_{\mathbf{r}^c}=\nabla^2\rho^{(p)}(\mathbf{r})|_{\mathbf{r}^c}+\nabla^2\rho^{(u)}(\mathbf{r})|_{\mathbf{r}^c}\neq 0$ which is not positive/negative defined.

The necessary complement for the local formalism presented above to complete the description of the electron structure is the *non-local* or *integrated formalism* within its topologic form. It introduces the quantum global descriptors determined by the integration of the densities, the further partition of the number of particles, and the corresponding associate magnitudes to the classical chemical concepts like atomic charges, covalent bond orders, valences, etc.[25,35] The nature of the information contained in these quantities or topologic population analysis is supported in the QTAIM of Bader's theory.[25,35] The multiatomic magnitudes within the present approach, which are relevant to our study, are the covalent bond order (two-center bond populations), $I_{\Omega_A\Omega_B}$ and the three-center bond population contributed by all possible populations shared by three centers, $I_{\Omega_A\Omega_B\Omega_C}$ defined by[24,25,36,37]

$$I_{\Omega_A\Omega_B}=\sum_{i,j,k,l} {}^1D_j^i\ {}^1D_l^k\ S_{il}(\Omega_A)\,S_{kj}(\Omega_B) \tag{3}$$

and

$$\begin{aligned}\Delta^{(3)}_{\Omega_A\Omega_B\Omega_C}&=\frac{1}{4}\sum_{P(\Omega_A\Omega_B\Omega_C)} I_{\Omega_A\Omega_B\Omega_C}\\&=\frac{1}{4}\sum_{P(\Omega_A\Omega_B\Omega_C)}\sum_{i,j,k,l,m,n} {}^1D_j^i\ {}^1D_l^k\ {}^1D_n^m\,S_{in}(\Omega_A)\,S_{kj}(\Omega_B)\,S_{ml}(\Omega_C)\end{aligned} \tag{4}$$

respectively, where Ω_A and Ω_B are the Bader's atomic domains in the physical space,[4,5] ${}^1D_j^i$ the matrix elements of spin-free first-order reduced density matrix as well as $S_{ij}(\Omega_A)$ those of the overlap matrix over the Ω_A physical domain in the orthonormal molecular basis set $\{i,j,k,l,\ldots\}$.[24,36,37] $P(\Omega_A\Omega_B\Omega_C)$ stands for the permutations over the domain contributions. The mono-atomic magnitudes of importance for our work are the effectively unpaired population, which quantifies the unpairing or break-down of the electron pairing due to correlation effects and/or spin multiplicity[24,32,33] and the unshared population for an atom *A*, Q_{Ω_A}, which are defined by

$$\begin{aligned}u_{\Omega_A}=2\sum_{ik} {}^1D_k^i\,S_{ik}(\Omega_A)-\sum_{ijkl} {}^1D_l^i\,{}^1D_k^j\,S_{ik}(\Omega_A)\,S_{ji}(\Omega_A)\\-\sum_{B\neq A}\sum_{ijkl} {}^1D_l^i\,{}^1D_k^j\,S_{ik}(\Omega_A)\,S_{ji}(\Omega_B)\end{aligned} \tag{5}$$

in which spin state contribution to that quantity is not present in this study because the systems are considered in their singlet ground state, and

$$Q_{\Omega_A}=\left[I_{\Omega_A\Omega_A}-\frac{1}{2}\sum_{\Omega_B\neq\Omega_A} I_{\Omega_A\Omega_B}\right]+\frac{1}{2}u_{\Omega_A} \tag{6}$$

whose physical meaning stands for the inner shells and/or lone pairs population in the atom, that is, the electrons that are not involved in bonding interactions.[25,35] The first and second terms represent the pairing contributions while the third one stands for the unpaired population contribution to this magnitude. The atomic nonshared populations Q_{Ω_A} and $I_{\Omega_A\Omega_B}$ covalent bond orders permit to express the contributions of the total population of each atom in the molecule in terms of their basins or domain occupations, that is, $N=\sum_{\Omega_A} N_{\Omega_A}$, as[35]

$$N_{\Omega_A}=Q_{\Omega_A}+\sum_{\Omega_B\neq\Omega_A} I_{\Omega_A\Omega_B} \tag{7}$$

where the last term of the r.h.s. of *Equation* 7 represents the shared population between the atom A and the rest of the system, that is, the sum of covalent bond orders.

3 | COMPUTATIONAL DETAILS, RESULTS AND DISCUSSION

3.1 | Preliminary details

The computational model in this work has been supported by state functions calculated at the level of approximation of configuration interaction with single and double excitations (CISD) in the basis sets 6-311G** using the Gamess package version 2013 (R1)[38] with *p* and *d* polarization functions for C and H atoms while the metal atoms incorporates the corresponding $(2d,f)$ functions. The geometrical structures were optimized within this approximation and have been confirmed to be local minimum for the energy. The densities, their critical points and their Laplacian fields $\nabla^2\rho^{(p)}(\mathbf{r})$ and $\nabla^2\rho^{(u)}(\mathbf{r})$ were calculated by AIMPAC modules.[39] The local concentration (accumulation or depletion) of the number of electrons at the point **r** of physical space has been described for practical reasons, by the $L(\mathbf{r})=-\nabla^2\rho(\mathbf{r})$ function, that is, accumulation (positive values) or depletion (negative values). The critical points of $\rho^{(u)}(\mathbf{r})$ which will be used in this study, are only those associated with its valence shell (vs). This is due to the fact that they

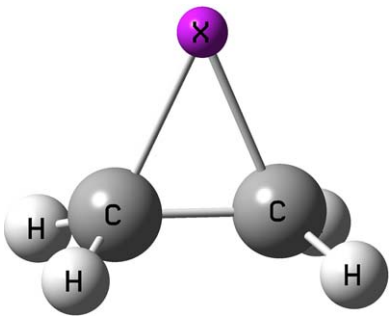

FIGURE 1 Geometrical structure of $X(C_2H_4)$ $(X = Ni, Cu^+, Zn^{2+})$

are mainly involved in bonding phenomena and no reference will be made to those of the inner shells unless exceptionally were part of the bonding interactions.[6,8,10] We will reserve the terms local accumulation and local depletion for the description of the densities.[4–6,40] The terminology *vscp* is used to refer to valence shell critical points of $\rho^{(u)}(\mathbf{r})$ with the same rank and signature of that of $\rho(\mathbf{r})$ in analogy with the ncp, bcp, rcp, and ccp's of the total density. It is important to note that such points are not *sensu strictu* bcp, rcp, or ccp's because only those of the total density define bonding interaction in the QTAIM topological formalism.[4,5]

Figure 1 shows the molecular structure scheme for the TM-L compounds ($Me^{p+}-L$). The corresponding geometrical parameters for each system which will be used throughout the discussion, are reported in Table 1. In the same way, the magnitudes (electron pairing and unpairing densities) describing the electron distribution are shown in Tables 2–4.

Table 2 collects the data featuring the electron density of each system from the topologic (local and nonlocal) point of view providing the electron structure of the molecules involved within this study. The paired density $\rho^{(p)}(\mathbf{r})$ is not presented there because as shown in our previous studies, its structure is similar to that of $\rho(\mathbf{r})$ and therefore, it does not introduce any new information.[6,10] The topologic electron structure of $\rho^{(u)}(\mathbf{r})$ and its associated chemical descriptors populations u_Ω, Q_{Ω_A}, and N_{Ω_A} are shown in Table 3. Table 4 shows the numerical values for each density and its $L(\mathbf{r})$ field at bcp's and vs(3,-1)cp's; and the ellipticity descriptor.[4,5,41]

3.2 | Electronic structure and density topology

The first necessary task to be done before performing the analysis and discussion of the results, is to establish of clear form, that the central feature of the type of phenomena treated in this work is the charge transfer, the associated electron population rearrangements and the contingent onset of complex patterns for atomic interactions expressed in terms of density contributions (cf. *Equation* 1). The magnitudes defined in the previous Section within the topologic formalisms will be employed to describe these features and to discuss the bonding interactions involved.

The pivotal idea to the discussion of the results collected in the Tables and Figures about the phenomena we are dealing with, is as follows: the Me^{p+}-L interaction is essentially based in the π cloud distribution at the CC sequence[11,12] which becomes modified by the interaction with the metal and the onset of complex patterns of bonding due to these changes. This will be the main task of our work. To achieve this goal, we search the details of these changes for the three chosen systems aforementioned.

The topologic structure of the total density ρ shown in Table 2, exhibits one **ncp** located on each nucleus for all systems, as it was expected. The essential differences between the systems, begin to be explicit through the study of **bcp**s. All systems present one **bcp** for CC and all CH sequences in the ligand with different density values at the CC **bcp** for Ni system, which are lower than that corresponding to Cu^+ and Zn^{2+} (see Table 4). The main and significant differences in the electronic structure of these systems resides in the onset and localization of some **bcp**s. The Ni-L system exhibits one **bcp** for each of the two NiC sequences, as well as one **rcp** for the CNiC sequence. In contrast, there are no **bcp**s between the metal atom and the C atoms for Cu^+, Zn^{2+} systems; however, the metal-ligand interaction is observed from the existence one **bcp** for the Me and CC middle point, that is, π cloud in molecular orbital terms.[11]

These results perfectly agree with covalent bond order I_{MeC} values of 0.910, 0.371, and 0.415 for Ni, Cu^+, Zn^{2+} systems, respectively, which complement the local topologic description of the MeC interaction. The covalent bond orders I_{CC} indicate a single bond (1.07) for the Ni interaction case, while intermediate values, of 1.572 and 1.466 arise for Cu^+ and Zn^{2+}, respectively, as shown in Table 2, that is, nor single neither double classical bonds appear for the CC interaction with these later metals. These results are also in agreement to the density values at their corresponding CC **bcp** observed in Table 4, which are lower for the Ni system in comparison with that of the other metals with higher CC covalent bond orders. These features are related to the geometrical conformation (Table 1) and the changes that the electron cloud of the

TABLE 1 Conformational parameters of the metal-ethylene complexes $Me^{p+}(C_2H_4)$ $(Me=Ni, Cu^+, Zn^{2+})$ at optimized geometry in the CISD/6-311G** level of approximation[a]

System	d(CC)[b]	d(Me $^{p+}$ C)[b]	d(CH)[b]	α(HCH)[c]	α(CMe $^{p+}$ C)[c]	D(HCCMe)[d]
Ni	1.45	1.83	1.09	112.3	46.7	108.7
Cu^+	1.36	2.12	1.08	117.1	37.3	96.5
Zn^{2+}	1.38	2.26	1.09	118.1	35.7	95.5

[a]Distances are expressed in Ångströms and angles in degrees.
[b]Sequence CC, CMe, CH distances.
[c]Planar angles.
[d]Dihedral angle between HCC and CCMe plane.

TABLE 2 Electronic Structure of metal-ethylene complexes $Me(C_2H_4)$ $(Me=Ni, Cu^+, Zn^{2+})$

cp Type	ρ sequences[a]	Bond	$I_{\Omega_A\Omega_B}$	$\Lambda^{(3)}_{\Omega_A\Omega_B\Omega_C}$
	Ni			
ncp	one on each nucleus			
bcp[b]	one at the CC sequence	CC	1.070	
	one for each CH sequence	CH	0.970	
	one for each CNi sequence	CNi	0.910	
rcp	one for the CNiC sequence	CNiC		0.093
ccp	no present			
	Cu^+			
ncp	one on each nucleus			
bcp[b]	one at the CC sequence	CC	1.572	
	one for each CH sequence	CH	0.933	
	no present for the CCu sequences	CCu	0.371	
	one for Cu-π cloud			
rcp	no present	CCuC		0.235
ccp	no present			
	Zn^{2+}			
ncp	one on each nucleus			
bcp[b]	one at the CC sequence	CC	1.466	
	one for each CH sequence	CH	0.895	
	no present for the CZn sequences	CZn	0.415	
	one for Zn-π cloud			
rcp	no present	CZnC		0.371
ccp	no present			

Local and integrated (nonlocal) topological features of $\rho(\mathbf{r})$ density at CISD/6-311G** level of approximation. All quantities are in atomic units.
[a]Indicate the nucleus at which the **ncp** is located; for **bcp**s, the atoms defining the bond; for **rcp**s, the atoms giving rise to the ring; for **ccp**s, the atoms defining the cage.
[b]Each bcp reported indicates also the existence of the corresponding bond path between these atoms both defining the bond, otherwise it will be specified in the text.

ligand undergoes due to the interaction with the metal of each system. Let us analyze these changes by means of the ellipticity ε (cf. Table 4) before discussing the flux of charge and the complex patterns within the electron distribution. The ellipticity is a local parameter defined by the relation of the values of the perpendicular curvatures to the bond path $\epsilon=(\lambda_1/\lambda_2)-1$ at a **bcp**.[4,5] In the case in which both curvatures are similar, the ellipticity equals to zero and the density around the **bcp** shows a cylindrical symmetry which is typical of a single homonuclear bond. For instance, $\lambda_1=\lambda_2=-0.4519$ for C_2H_6 system at the present level of approximation. Its most known interpretation is related to provide a measure for the anisotropy of the charge distribution around the corresponding **bcp**.[41] The geometric parameters shown in Table 1 indicate that the ligand C_2H_4 abandons its flat shape and enlarges its d_{CC} distance. This feature is present in all systems although the more marked structural changes in the ligand system are produced in the Ni system, that is, the loss of planarity by 18.7 degrees and the enlargement of the d_{CC} distance from the isolated C_2H_4, $\approx$ 1.33 to 1.45Å. This distortion induces a $\varepsilon=0.25$ (Table 4) which is typical to an intermediate interaction between a single and a double bond[4] and supported by the I_{CC} value close to 1 as discussed above. As it may be observed from the Tables 1 and 4, the remaining systems, Cu^+ and Zn^{2+} show that the ligand deviates slightly from planarity (6.5 and 5.5 degrees, respectively) and d_{CC} distances of 1.36 and 1.38Å, are closer to what is a double bond. Therefore, intermediate (no integer) values for I_{CC}s which are different from 1 (single bond) and 2 (double bond) are in agreement with these distances. It indicates that the π cloud becomes distorted but never broken as in the Ni system. Nevertheless, the ellipticity merits a further interpretation because even we expect greater values for the ellipticity of Cu^+, Zn^{2+} systems respect that of Ni because of their similar structural features (d_{CC} and D(MeCCH) in Table 1) and the nonbroken character of the π cloud, the ellipticity for Zn^{2+} (0.16) is lower than that of Ni. This ellipticity lowering arises from the decrease of λ_1 (−0.68) curvature and the increase of λ_2 (−0.58), this last one corresponding to the eigenvector inside the CMeC plane and perpendicular to the CC bond path. Therefore, this ellipticity lowering may not be interpreted as coming only from the broken π cloud of the CC sequence but also due to the constitution of a stronger Me-π cloud interaction as other source of anisotropy.

3.3 | Charge rearrangements and interaction's nature

Regarding the changes described above, let us inspect the charge transfer between different parts of the molecule by the analysis of the atomic populations in Table 3. In the $Ni(C_2H_4)$ system, the total population $N_{\Omega_{Ni}}$ is 27.361, which is less than 28 (Ni atomic number) indicating that it becomes positively charged. Hence it has undergone a charge transfer of donor type. Something similar may be noted for the lowering of I_{CC} in C_2H_4 ligand which becomes close to 1.0; considering that for an isolated C_2H_4 it is expected an I_{CC} of approximate 2.0, it can be inferred that the π cloud is missing and then the ligand acts like a donator of electrons in the same manner as the metal do. These population rearrangements, the existence of **bcp** and the I_{NiC} value as well as the charge accumulation within the NiC internuclear region shown in Figure 2a permit to infer the formation of a single bond between the metal and each of the C atoms. The other two systems, as well as in the Ni case, are also positively charged with atomic populations of 28.214 and 28.560 for Cu^+ and Zn^{2+} which indicate charges of 0.786 and 1.440 for each atom, respectively. These charges are close to 1 and 2 (their apriori oxidation states) which show that the Cu and Zn preserve their ion structure and are not able to provide electrons as the Ni atom. Moreover, the π cloud is weakened as indicated by I_{CC} and ellipticity values mentioned in the above paragraph. Hence, no single but intermediate bonds (fractional covalent bond orders) appear between the Me and the C atoms, that is, there is not enough electron population displacement from the CC π cloud toward the MeC internuclear regions to form bonds as in the Ni system case.

At this stage, once clearly established the existence of a bonding interaction between the Ni and the C atoms, a question is imposed, which is the nature of the NiC interaction? what type of atomic

TABLE 3 Electronic structure of metal-ethylene complexes $Me(C_2H_4)$ ($Me = Ni, Cu^+, Zn^{2+}$)

cp Type	$\rho^{(u)}$ Sequences[a]	Atom	Q_{Ω_A}	u_{Ω_A}[b]	N_{Ω_A}
	Ni				
vs (3,-3) cp	one on each of the nucleus	Ni	25.329	0.428	27.361
		C	2.150	0.160	6.165
		H	−0.045	0.060	1.070
vs (3,-1) cp	one for the CC sequence				
	one for each CNi sequence				
	one per each of CH sequence				
vs (3,+1) cp	one for CNiC sequence				
vs (3,+3) cp	no present				
	Cu^+				
vs (3,-3) cp	one on each of the nucleus	Cu	27.393	0.387	28.214
		C	2.135	0.146	6.051
		H	−0.130	0.047	0.920
vs (3,-1) cp	one for the CC sequence				
	one for each CCu sequence				
	one per each of CH sequence				
vs (3,+1) cp	one for CCuC sequence				
vs (3,+3) cp	no present				
	Zn^{2+}				
vs (3,-3) cp	one on each of the nucleus	Zn	27.672	0.335	28.560
		C	2.339	0.147	6.100
		H	−0.176	0.043	0.811
vs (3,-1) cp	one for the CC sequence				
	one for each CZn sequence				
	one per each of CH sequence				
vs (3,+1) cp	one for CZnC sequence				
vs (3,+3) cp	no present				

Local and integrated (nonlocal) topological features of $\rho^{(u)}(\mathbf{r})$ density at CISD/6-311G** level of approximation. All quantities are in atomic units.
[a]Indicate the nucleus at which the **vs(3,-3)cp** is located; for **vs(3,-1)cp**s, the atoms defining the corresponding sequence; for **vs(3,+1)cp**s, the atoms giving rise to the ring; for **vs(3,+3)cp**s, the atoms defining the cage.
[b]Effectively unpaired atomic electron population.

interaction is present at the NiC sequence? Analyzing the trends of the Laplacian fields and their values at the NiC **bcp**, it may be noted (cf. Table 4) that both densities paired (resembled by the total density as explained above) and unpaired, deplete in the internuclear space. Therefore, it means that both densities tend to concentrate in the atomic core domain, that is, near the nuclei. They may be considered as a closed-shell interaction.[4]

It seems to occur for typical ionic interactions and for an intermediate interaction between the pure covalent and ionic interactions of the often called *charge-shift bond* (CSB) or deficient covalent bond type.[42–44] These two types of atomic interactions can be differentiated within the density view, according to the electron population that each atom houses. Let us compare for that goal, the present NiC case with that of the ionic NaCl.[9] Table 4 reports the density and the unpaired density depletion with −0.292 and −0.007 values for the $L(\mathbf{r})$ function at the **bcp** for Ni and C, respectively (cf. Figure 2d for a graphical view). For the same level of approximation, −0.191 and −0.001 values are obtained for Cl and Na, respectively. Hence, these numbers do not help us to decide what type of bonding interaction is present in NiC sequence because they are similar. The integrated magnitudes reported in Tables 2 and 3 indicate electron charges of 0.639, −0.165 for Ni and C, respectively. For the typical ionic NaCl charges of 0.900, −0.900 were obtained for Cl and Na atoms, respectively. Further, a 0.910 covalent bond order $I_{\Omega_A\Omega_B}$ (cf. Table 2) is calculated for NiC, close to the ideal single covalent bond order (1.0), while a low 0.222 value for NaCl. Finally, let us note that for Ni system there are a $\rho^{(u)}$ spillage through the internuclear NiC line (cf. Figure 2d) while it does not appear for ionic NaCl (cf. Ref. [8]). Therefore, from this analysis it is right to state that the NiC interaction is of CSB type because as shown above, the electronic descriptors clearly indicate that the interactions are neither covalent nor ionic ones but intermediate with a marked depletion of the electron density.[42–44]

TABLE 4 Total ρ and unpaired $\rho^{(u)}$ densities and their $L(\mathbf{r})$ function for metal-ethylene complexes $Me(C_2H_4)$ $(Me = Ni, Cu^+, Zn^{2+})$ at bond critical points of the total density at CISD/6-311G** level of calculation[a]

System[b]	Bond	$\rho(\mathbf{r})\|_{bcp}$	$\rho^{(u)}(\mathbf{r})\|_{bcp}$	$-\nabla^2\rho(\mathbf{r})\|_{bcp}$	$-\nabla^2\rho^{(u)}(\mathbf{r})\|_{bcp}$	ε[c]
$Ni(C_2H_4)$	CNi	0.1459	0.0034	−0.2915	−0.0067	0.3991
		0.1456	0.0034	−0.3213	−0.0076	0.0756
	CC	0.2793	0.0041	0.7190	−0.0081	0.2458
		0.2792	0.0041	0.7146	−0.0082	0.2997
	CH	0.2744	0.0036	0.9295	−0.0053	0.0475
		0.2743	0.0036	0.9280	−0.0056	0.1649
	rcp CNiC sequence	0.1277	0.0025	−0.5201	−0.0109	
		0.1297	0.0025	−0.3993	−0.0107	
$Cu^+(C_2H_4)$	CCu[d]					
		0.0737	0.0018	−0.1508	−0.0026	0.2021
	CC	0.3344	0.0045	1.0178	−0.0106	0.3151
		0.3343	0.0045	1.0167	−0.0106	0.4931
	CH	0.2879	0.0037	1.0414	−0.0062	0.0127
		0.2875	0.0037	1.0371	−0.0061	0.1255
	rcp CCuC sequence[e]					
		0.0816	0.0016	−0.1515	−0.0052	
	Cu−π cloud[f,g]	0.0791	0.0017	−0.2218	−0.0048	5.9162
$Zn^{2+}(C_2H_4)$	CZn[d]					
		0.0578	0.0013	−0.0722	−0.0027	0.3520
	CC	0.3249	0.0045	1.0036	−0.0103	0.1634
		0.3249	0.0045	1.0035	−0.0103	0.3844
	CH	0.2887	0.0037	1.0761	−0.0055	0.0083
		0.2887	0.0037	1.0526	−0.0059	0.0730
	rcp CZnC sequence[e]					
		0.0657	0.0012	−0.0856	−0.0043	
	Zn−π cloud[f,g]	0.0629	0.0012	−0.0931	−0.0035	2.2303

All quantities are in atomic units.
[a]Second line in Columns 3 to 7 for each sequence, indicates the densities and $L(\mathbf{r})$ at $\rho^{(u)}(\mathbf{r})$ vs(3,-1)cp and vs(3,+1)cp.
[b]See Figure 1 for atoms labeling.
[c]Ellipticity.
[d]There are no bcp points for $\rho(\mathbf{r})$ between these atoms.
[e]There are no rcp points for $\rho(\mathbf{r})$ for this sequence.
[f]Corresponding at the bcp between the Me^{p+} and the CC sequence (cf. Figure 2).
[g]There are no $vs(3,-1)$cp's of $\rho^{(u)}(\mathbf{r})$ for this sequence.

The fundamental differences between both types of Me-L interactions presented in this study are that for the interaction of the Ni atom with L is described by the existence of one **bcp** at each of both CNi sequences which indicate bonding interactions between these atoms, and one **rcp** defined by the CNiC sequence which defines a ring structure. Both type of interactions set the electronic structure of $Ni(C_2H_4)$. In the other systems, the ion metals Cu^+ and Zn^{2+} exhibit only a global type of interaction with L, expressed by the onset of only one **bcp** showing a strong Me−π cloud bonding interaction and a depletion for both fields at this **bcp**. This depletion of both densities at that interatomic regions constitutes a typical closed-shell interaction. The CC and CH sequences exhibit paired field accumulation and unpaired field depletion at **bcp**s for all systems, typical of a covalent interaction (shared interaction),[9] as it was expected within the carbonyl ligand.[4] Figure 2 shows in a graphic manner the different trends for the total and the unpaired densities, Figures 2a–2c and 2d–2f, respectively. The NiC sequence enlarges its pairing density (accumulates) in the internuclear region as explained above, while it becomes depleted for the other MeC system sequences. This is in agreement with the values for the bond orders discussed above. Unpaired populations u_Ω are similar for all metals showing a nonsaturated capacity for accepting electrons (hole populations)[24] as well as the C atoms, while it is clearly diminished for H atoms (cf. Table 3).

The above discussion of the charge transfer and the bond formation (strength of the bonding interaction under the existence of **bcp**s) permit to establish that the Ni system is the one that undergoes a back-donation interaction while remaining systems do not.

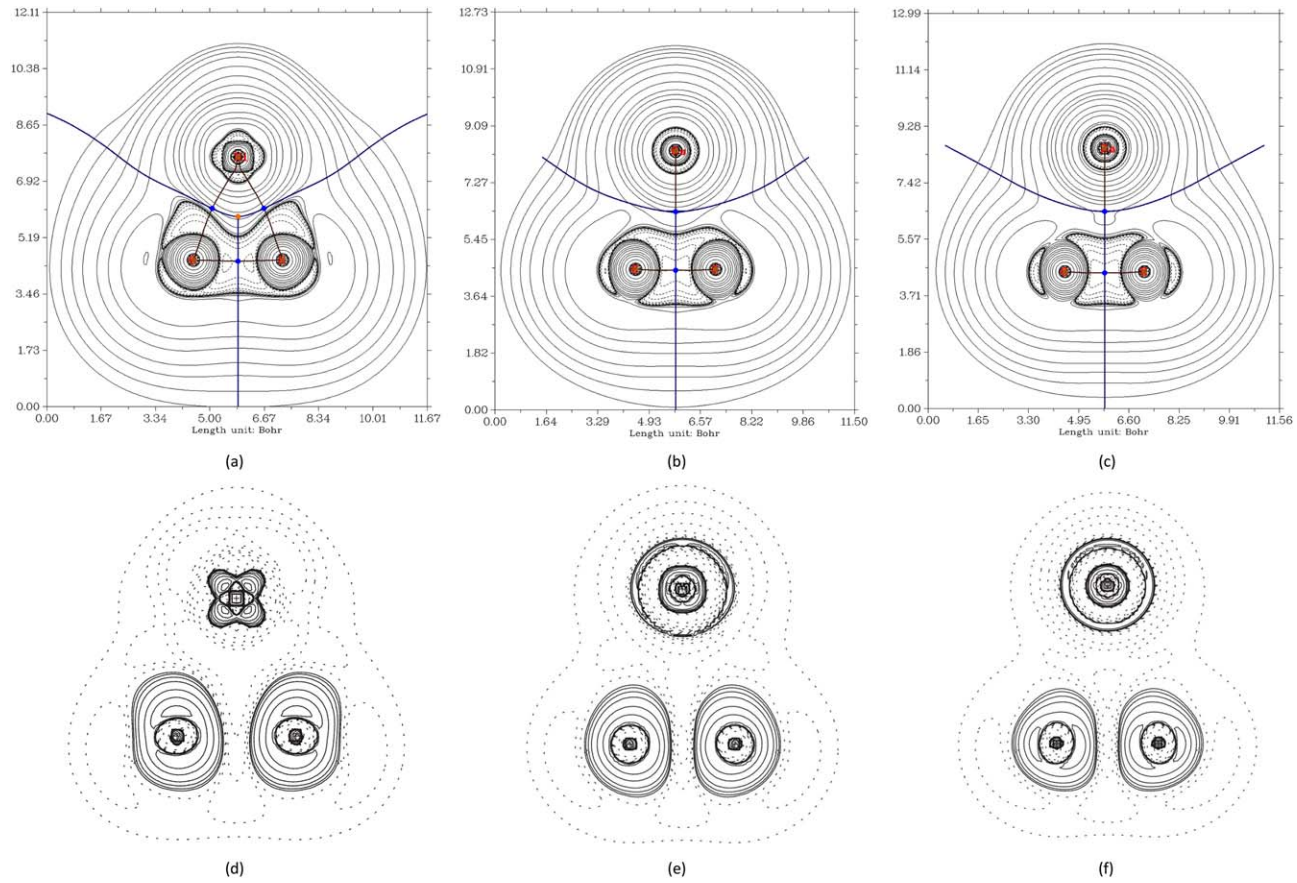

FIGURE 2 $L(\mathbf{r})$ contour maps for total density (a, b, and c) and effectively unpaired densities (d, e, and f) for $X = Ni, Cu^{+}, Zn^{2+}$, respectively, in the plane defined by CXC atoms (see Figure 1). Positive and negative values are denoted by solid and dashed lines, respectively

3.4 | Complex interactions and back-donation phenomena

Let us inspect the remaining information contained in the electronic distribution to search for complex patterns of bonding interactions between the atomic domains. Therefore, it leads us beyond the traditional chemical descriptors discussed up to now. For that goal, we perform the analysis of the 2e-3c populations $\Delta^{(3)}_{\Omega_C\Omega_{Me}\Omega_C}$ and the information contained in $\rho^{(u)}$.[6,8–10] These populations which are reported in Table 2 show that they are significantly lower for the Me–L interaction in the case for Ni (0.093) in comparison to those for Cu^{+} and Zn^{2+}, 0.235 and 0.371, respectively. The existence of one **rcp** for the CNiC sequence is coincident with its lowest 2e-3c population and the complete broken π cloud. The I_{CH} bond orders in each system follow an opposite trend, that is, they diminish as the 2e-3c populations increase. No **ccp**s exist for such interactions in the systems presented; this is an expected result because the systems could posses a ring but no a cage structure. Finer details of the electron distribution are hidden in the unpaired density $\rho^{(u)}$ and its analysis reveals them. The results are condensed in Tables 3 and 4.

Table 3 shows that all nuclei in the systems present a maxima vs(3,-3)cp close to the nuclear positions. All sequences MeC, CC, and CH show vs(3,-1)cp as well as a vs(3,+1)cp formed by the CMeC sequence (note that only for Ni there is one **rcp**). The values for ρ, $\rho^{(u)}$, as well as their Laplacian fields, are very similar when evaluated at their corresponding **bcp** and vs(3,-1)cp, respectively (cf. Table 4), that is, the cp's and the vscp's are very close each other.[6,8–10] Moreover, it may be noted that the Ni system does not follow the nonlocal part of the quantum rule for the existence of a 2e-3c interactions[45] (A 2e-3c bond between atoms ABC exists if there is a vs(3,-1)cp of $\rho^{(u)}$ between each pair of atoms involved in the three-center ABC sequence and a vs(3,+1)cp defined only by the atoms involved in the three center sequence (local rule). The integrated or nonlocal rule states that the existence of a 2e-3c bond between atoms ABC is when fractional covalent bond orders $I_{\Omega_A\Omega_B}$ appear between all possible pairs of atoms AB, BC, AC and an appreciable $\Delta^{(3)}_{\Omega_A\Omega_B\Omega_C}$ which defines its strength).[6] Even more, it becomes clear from Table 2, that this system is described by 2e-2c distributions, that is, the atomic interactions are reduced to a set of 2e-2c ones as in the most of the classical atomic interactions, and so consequently it does not undergo 2e-3c interactions. The other systems, those of Cu^{+}, Zn^{2+}, fulfill the topologic conditions of the rule (local and nonlocal) and consequently they undergo 2e-3c atomic interactions. Figure 2d–2f show the $\rho^{(u)}$ accumulation in space around the metal nuclei. The Ni system shows a leading *d*-type symmetry shape, while for Cu^{+} and Zn^{2+} the local accumulation around them shows a spherical symmetry, that is, *s*-type.

At this point, the results obtained from the analysis of the electron distribution of the systems allow us to note some crucial relationships

between these interactions and the concept of back-donation introduced in the first section.[11]

The back-donation charge has been defined, in the orbital picture, by orbital selection of different sets corresponding to each isolated domains, that is, both parts, Me and L donate and accept charge at the same time.[11,12] Nevertheless, from the point of view of the density it may be interpreted in a distinct way considering that both parts, that is, the Me and the L donate or accept charge as part of the interaction process forming bonds. These concepts are described by means of the electron populations defined in the previous section. As it is well known, the back-donation phenomena is explained through the interaction of metal valence electrons with the π cloud of the ligand.[11–13,45] Namely, to properly describe the rearrangements of the whole system Me-L in comparison with their isolated structures, it must be described how the Me and the L become modified. For that goal, it may noted that two different features arise. In the Ni system, the π cloud distribution disappears as explained above and thus the electron structure of L is severely modified, while the metal also contribute donating charge (cf. its total population from Table 3). Hence, both the metallic Ni and the ligand contribute enough electrons to create CNi bonding interactions as indicated by the onset of one **bcp** at each of the NiC sequences. In the other two systems, the metals are more electrically charged than the Ni, thus preserving their ion structure, that is, their *a priori* oxidation states + 1 and + 2 for the Cu and Zn atoms, respectively, and the π cloud in the ligand is slightly perturbed. Then, these latter systems do not transfer enough charge which is not able to form **bcp**s and consequently, MeC interaction is weak. However, their charge rearrangement produce a Me−π interaction as indicated by the appearance of one **bcp** placed between the metal and the line joining the CC sequence midpoint besides the electron density accumulation at this point (cf. Figure 2b–2c).

The results discussed in the previous paragraph have shown that in all systems both domains, that is, the Me and L, donate electrons. Nevertheless, only the systems with bonding interactions characterized by the appearance of **bcp**s between the Me and the C atoms in the ligand undergo back-donation phenomena. Thus, this feature is the key indicator for such phenomena from the viewpoint of the density. So that, the Ni system undergoes back-donation, while the Cu^+, Zn^{2+} systems do not. Then the system which undergoes back-donation phenomena, that is, Ni, cannot support 2e-3c interactions as noted above. In contrast, those systems which do not undergo back-donation show 2e-3c interactions. It is worthy to note that the topologic structure of the type shown in Figure 2b–2c, that is, with one **bcp** located between the Me and the π cloud are denominated as *T*-shaped.

3.5 | Density-based chemical descriptors for back-donation

To complete the discussion, we introduce a proposal for back-donation population indicator as an electron magnitude descriptor based in the population magnitudes introduced in the second Section, that is, which revels the density point of view. For that purpose, let us first comment the two visions of this phenomena, that coming from orbital theories[11] and the present one supported by the electron density itself. On one side, the orbital view invokes an orbital interaction, or in mathematical sense a linear combinations of a d_{z^2} (d_{yz}) orbital of the Me and a molecular orbital of the ligand, σ (σ^*) or π (π^*) of *L*, giving rise to two molecular orbitals describing the Me–L (cf. figure 9 of Ref. [45]) interaction. On the other side, that from the density view, no molecular orbitals combinations are used. Hence, it is no possible to adjudicate from which orbital the charge flux occurs between the Me and the L, then this analysis is transferred into the concept of density accumulation/depletion and the onset of **bcp**s to determine the type of Me–L bonding interaction. Hence, to proceed for counting the populations, we define the following magnitudes as

$$N_L=\sum_{\Omega_A \epsilon L} N_{\Omega_A},\ Z_L=\sum_{\Omega_A \epsilon L} Z_{\Omega_A} \tag{8a}$$

$$\bar{N}_L=N_L-2\sum_{\Omega_A \epsilon L} I_{\Omega_A \mathrm{Me}},\ \bar{N}_{\mathrm{Me}}=N_{\mathrm{Me}}-2\sum_{\Omega_A \epsilon L} I_{\Omega_A \mathrm{Me}} \tag{8b}$$

$$\Delta_d^L=Z_L-\bar{N}_L,\ \Delta_d^{\mathrm{Me}}=Z_{\mathrm{Me}}-\bar{N}_{\mathrm{Me}} \tag{8c}$$

where the sums are restricted to the atoms forming the ligand ($\Omega_A \epsilon L$); N_L, Z_L (*Equation* 8a) and $\bar{N}_L$ (formula in the left side of *Equation* 8b) stand for the total population, the atomic number (with Z_{Ω_A}, the atomic number of atom A) and the nonshared population of L with the metal, that is, its total population minus the shared ($2I_{\Omega_A \mathrm{Me}}$, because each atom provide charge symmetrically) population[35] of L and Me, respectively. The $\bar{N}_{\mathrm{Me}}$ (formula in the right side of *Equation* 8b) has the same physical meaning for the metal with atomic number Z_{Me}, as $\bar{N}_L$ for the ligand. Allow us to note that the population $\bar{N}_{\mathrm{Me}}$ of the metal (on the right side of Equation 8b) does not have any indication regarding the ligand because this is unique and does not lead to misunderstanding. Finally, the magnitudes Δ_d^L and Δ_d^{Me} (*Equation* 8c) represent each donation (or back-donation) charge within the system, that is, the values of the promoted populations from the Me and L, respectively. The calculated values for Δ_d^{Me}; Δ_d^L are approximately 2.60, 1.20; 0.5, 1.00 and 0.30, 1.40 for Ni, Cu^+, Zn^{2+} metals and ligand, respectively. These values indicate that the metal is the driving force for back-donation. The only system between those presented here undergoing this phenomena as discussed above, is the $Ni(C_2H_4)$ in which the metal provides enough charge to build bonding interactions featured by the onset of the **bcp** between the metal and the C atoms of the ligand and the **rcp** of the CNiC sequence (see Table 2). This is in agreement with the fact that the Ni is the only metal whose oxidation state become modified while the others tends to preserve it as discussed above and may not provide enough electrons to interact with the π cloud to form bcps between the Me and the C atoms. The physical meaning of the sum of both donation charges, $\Delta_d^L+\Delta_d^{\mathrm{Me}}=N-(\bar{N}_L+\bar{N}_{\mathrm{Me}})$ is the number of electrons directly involved in the Me–L interaction. In the case of Ni system, it is close to 4.0, that is, the number of two pairs of electrons expected to form two classic NiC bonding sequences. For the remaining systems, Cu^+ and Zn^{2+} these populations are approximately 1.5 and 1.7, respectively, and result not enough to define the MeC **bcp**s.

4 | CONCLUDING REMARKS

In this report, the back-donation phenomena is described and analyzed from the density point of view. For that goal, we used three metallic isoelectronic series, namely, Ni, Cu^{+}, and Zn^{2+} interacting with one ethylene molecule as ligand. These systems provide the most important features to understand the mentioned phenomena in terms of the weakening/strenghtening of the interactions between the atoms. According to the flux of charge observed in the calculations, when the system undergo back-donation, as it is for the Ni system case, the electronic structure may be described as formed by classical 2e-2c type interactions, while for the other systems which do not present back-donation, 2e-3c interactions arise. This result is of fundamental importance and the main one within this work because it seems that back-donation phenomena and 2e-3c interactions exclude themselves. It is worthy to note that, because density models are not based on the concept of orbital, they are unable to discriminate between σ and π contributions as orbital models do, at least in a direct manner but as shown in the discussion, the electronic structure reveal in an indirect way the existence of this type of symmetry distributions.

The 2e-3c atomic interactions were detected by means of the onset and localization of the $\rho^{(u)}$ density **vscp**s in view of a local and nonlocal topologic rule. This is an information that cannot be obtained from the total or the paired densities. This methodology has been successfully applied to simple organo-metallic systems, that is, systems with only one metallic-ligand structure interactions giving an accurate description of the electronic distribution. Also it may be remarked that the calculation of the electronic parameters discussed to quantify the back-donation populations (cf. Equations 8) are valid for any type of state function, because of the general validity of the used tools.

These important consequences from the detailed study for complex interactions between metallic atoms interacting with organic ligands providing a π cloud, give rise to different molecular structures, that is, some of them described by 2e-2c or 2e-3c interactions and constitute a natural scenario for the application of these techniques to complex systems with more than one ligand. This subject is under consideration in our laboratories.

ACKNOWLEDGMENTS

This report has been financially supported by Projects 20020130100226BA (Universidad de Buenos Aires) and PIP No. 11220090100061 (Consejo Nacional de Investigaciones Científicas y Técnicas, República Argentina). R. M. L. acknowledges financial support of the Secretaría General de Ciencia y Técnica de la Universidad Nacional del Nordeste (Corrientes, Argentina) and facilities provided during the course of this work. Part of the computations presented in this paper were performed using the CIMENT infrastructure, which is supported by the Rhône-Alpes region - France (Grant CPER07-13 CIRA).

REFERENCES

[1] A. S. Bamzai, B. M. Deb, *Rev. Mod. Phys.* **1981**, *53*, 95.

[2] A. J. Coleman, V. I. Yukalov, *Reduced Density Matrices: Coulson's Challenge*, Springer-Verlag, New York **2000**.

[3] R. G. Parr, W. Yang, *Density-Functional Theory of Atoms and Molecules*, Oxford University Press, New York **1989**.

[4] R. F. W. Bader, *Atoms in Molecules: A Quantum Theory*, Clarendon Press, Oxford **1994**.

[5] P. L. A. Popelier, *Atoms in Molecules: An Introduction*, Pearson Educ., London **1999**.

[6] R. M. Lobayan, R. C. Bochicchio, *J. Chem. Phys.* **2014**, *140*, 174302.

[7] R. F. W. Bader, *J. Phys. Chem. A* **2009**, *113*, 10391.

[8] R. M. Lobayan, R. C. Bochicchio, L. Lain, A. Torre, *J. Chem. Phys.* **2005**, *123*, 144116.

[9] R. M. Lobayan, R. C. Bochicchio, L. Lain, A. Torre, *J. Phys. Chem. A* **2007**, *111*, 3166.

[10] R. M. Lobayan, R. C. Bochicchio, *J. Phys. Chem. A* **2015**, *119*, 7000.

[11] G. Frenking, N. Fröhlich, *Chem. Rev.* **2000**, *100*, 717.

[12] G. Frenking, in *Modern Coordination Chemistry. The Legacy of Joseph Chatt* (Eds: G. J. Leight, N. Winterton), The Royal Society of Chemistry, Cambridge **2002**.

[13] J. Uddin, S. Dapprich, G. Frenking, B. F. Yates, *Organometallics* **1999**, *18*, 457.

[14] E. R. Davidson, K. L. Kunze, F. B. C. Machado, S. J. Chakravorty, *Acc. Chem. Res.* **1993**, *26*, 628.

[15] Y. Jean, *Molecular Orbitals of Transition Metal Complexes*, Oxford University Press, New York **2005**.

[16] S. Dapprich, G. Frenking, *J. Phys. Chem.* **1995**, *99*, 9352.

[17] K. Boguslawski, P. Tecmer, G. Barcza, Ö. Legeza, M. Reiher, *J. Chem. Theory Comput.* **2013**, *9*, 2959.

[18] M. Mottet, P. Tecmer, K. Boguslawski, Ö. Legeza, M. Reiher, *Phys. Chem. Chem. Phys.* **2014**, *16*, 8872.

[19] C. Duperrouzela, P. Tecmera, K. Boguslawskia, G. Barczab, Ö. Legezab, P. W. Ayers, *Chem. Phys. Lett.* **2015**, *621*, 160.,

[20] Y. Zhao, K. Boguslawski, P. Tecmer, C. Duperrouzel, G. Barcza, Ö. Legeza, P. W. Ayers, *Theor. Chem. Acc.* **2015**, *134*, 120.

[21] R. H. Hertwig, W. Koch, D. Schröder, H. Schwarz, J. Hrušák, P. Schwerdtfeger, *J. Phys. Chem.* **1996**, *100*, 12253.

[22] P. O. Widmark, B. Roos, P. E. M. Siegbahn, *J. Phys. Chem.* **1985**, *89*, 2180.

[23] F. Bernardi, A. Bottoni, M. Calcinari, I. Rossi, M. Robb, *J. Phys. Chem. A* **1997**, *101*, 6310.

[24] R. C. Bochicchio, L. Lain, A. Torre, *Chem. Phys. Lett.* **2003**, *375*, 576.

[25] L. Lain, A. Torre, R. C. Bochicchio, *J. Phys. Chem. A* **2004**, *108*, 4132.

[26] P. Macchi, A. Sironi, in *The Quantum Theory of Atoms in Molecules. From Solid State to DNA and Drug Design* (Eds.: C. F. Matta, R. J. Boyd), Wiley-VCH, Weinheim **2007**.

[27] E. D. Davidson, *Reduced Density Matrices in Quantum Chemistry*, Academic, New York **1976**.

[28] R. McWeeny, *Methods of Molecular Quantum Mechanics*, Academic, London **1969**.

[29] R. M. Lobayan, D. R. Alcoba, R. C. Bochicchio, A. Torre, L. Lain, *J. Phys. Chem. A* **2010**, *114*, 1200.

[30] K. Takatsuka, T. Fueno, T. K. Yamaguchi, *Theor. Chim. Acta* **1978**, *48*, 175.

[31] K. Takatsuka, T. Fueno, *J. Chem. Phys.* **1978**, *69*, 661.

[32] R. C. Bochicchio, *J. Mol. Struct. (THEOCHEM)* **1998**, *429*, 229.

[33] V. N. Staroverov, E. R. Davidson, *Chem. Phys. Lett.* **2000**, *330*, 161.

[34] D. R. Alcoba, R. C. Bochicchio, L. Lain, A. Torre, *J. Chem. Phys.* **2010**, *133*, 144104.

[35] R. C. Bochicchio, *J. Mol. Struct. (THEOCHEM)* **1991**, *228*, 209.

[36] X. Fradera, M. A. Austen, R. F. W. Bader, *J. Phys. Chem. A* **1999**, *103*, 304.

[37] A. Torre, L. Lain, R. C. Bochicchio, R. Ponec, *J. Math. Chem.* **2002**, *32*, 241.

[38] M. W. Schmidt, K. K. Baldridge, J. A. Boatz, S. T. Elbert, M. S. Gordon, J. H. Jensen, S. Koseki, N. Matsunaga, K. A. Nguyen, S. J. Su, T. L. Windus, M. Dupuis, J. A. Montgomery, *J. Comput. Chem.* **1993**, *14*, 1347.

[39] F. W. Biegler-König, R. F. W. Bader, T. H. Tang, *J. Comput. Chem.* **1982**, *3*, 317.

[40] P. L. A. Popelier, *Coord. Chem. Rev.* **2000**, *197*, 169.

[41] C. Silva López, A. R. de Lera, *Curr. Org. Chem.* **2011**, *15*, 3576.

[42] W. Wu, J. Gu, J. Song, S. Shaik, P. Hiberty, *Angew. Chem.* **2009**, *48*, 1407.

[43] R. M. Lobayan, R. C. Bochicchio, *Chem. Phys Lett.* **2013**, *557*, 154.

[44] Y. Yang, *J. Phys. Chem. A* **2012**, *116*, 10150.

[45] J. C. Green, M. L. H. Green, G. Perkin, *Chem. Commun.* **2012**, *48*, 11481.

How to cite this article: R. M. Lobayan, R. C. Bochicchio, C. Pérez del Valle *Int. J. Quantum Chem.* **2016**, 00: 000–000. DOI: 10.1002/qua.25285